Double-layered co-microencapsulated ammonium polyphosphate and mesoporous MCM-41 in intumescent flame-retardant natural rubber composites

Na Wang · Long Mi · Yuxian Wu · Jing Zhang ·
Qinghong Fang

Abstract Double-layered co-microencapsulated ammonium polyphosphate (APP) and mesoporous MCM-41 (M(A&M)) were prepared using melamine–formaldehyde resin and zinc borate by in situ polymerization. The structure of the microcapsules was characterized by particle size analysis, Fourier-transform infrared spectroscopy, and scanning electron microscopy. Double-layered microencapsulation gave APP narrow particle size distribution. The flame-retardant and mechanical effects of M(A&M) in natural rubber (NR) were evaluated using the limiting oxygen index, UL 94 test, thermogravimetric analysis, and tensile test. Results indicated that the NR/M(A&M) composites had much better flame-retardant and mechanical properties than the NR/APP/MCM-41 composites. The limited oxygen index value of the NR/M(A&M) composite reached the maximum, and the UL-94 ratings were increased to V-0 when the ratio of APP to MCM-41 was 39:1 in microcapsule. The occurrence of a synergistic effect between MCM-41 and intumescent flame-retardant in the NR composites was proved. This investigation provided a promising formulation for flame-retardant NR composites.

Keywords Double-layered microencapsulation ·
Intumescent flame retardant · Synergism ·
Mesoporous MCM-41 · Natural rubber

Introduction

Natural rubber (NR) is a material that presents certain unique advantages over competitive synthetic rubbers in many applications caused by the unique combination of its physico-mechanical properties. NR is particularly applied in a wide range of commercial products such as tires of aircraft and automotives that require superior properties. However, NR has a low limited oxygen index (LOI) and is easy to combust when ignited. Such inherent easy flammability prevents NR from being used in certain highly demanding applications such as coal mine conveyor belts and aircraft tire treads [1–3].

Flame retardants are usually added to overcome this problem. Halogenated flame retardants are often used to enhance the fire resistance of NR. However, the uses of these flame retardants are limited because of the potential environmental hazards and life safety issues that these retardants may cause. Hence, the development of novel halogen-free flame retardants is necessary. Intumescent flame retardants (IFRs) are receiving considerable attention [4, 5]. A typical and widely used IFR system is a mixture of ammonium polyphosphate (APP), pentaerythritol (PER), and melamine (MEL). IFR additives in NR should preferably have minimal smoke release and low toxicity during burning, particularly when used in further combination with other additives that lead to improved fire retardancy. Wang et al. [4] reported that the 4A zeolite can be an effective filler for improving the mechanical and flame-retardant (FR) properties of NR composites. Synergism has also been found between IFR and MCM-41 or SBA-15 in polypropylene (PP) composites (PP-IFR) in our previous work. Results show that mesoporous silica MCM-41 and SBA-15 exert the effective synergistic effect found in intumescent flame-retardant systems of PP to obtain good

N. Wang (✉) · L. Mi · Y. Wu · J. Zhang · Q. Fang
College of Materials Science and Engineering, Shenyang
University of Chemical Technology, Shenyang 110142, China
e-mail: iamwangna@sina.com

flame retardancy. MCM-41 and SBA-15 are also observed to have remarkable effects on mechanical properties compared with a PP/PP-g-MA/IFR system [6]. However, most IFR systems present certain problems such as moisture sensitivity and poor compatibility with NR or the polymer matrix because of the high polarity of the components [7]. Microencapsulation of the IFR system has been regarded as an effective strategy to overcome such problems. Hu Yuan et al. [8, 9] successfully microencapsulated APP (MAPP) with polyurethane (PU), urea-MEL-formaldehyde resin, and PVA-MEL-formaldehyde resin shell. To improve the FR properties of composites, carbon source dipentaerythritol (DPER)/pentaerythritol (PER) are co-microencapsulated with APP, and the co-microencapsulated APP and DPER/PER (M (A&D)/M (A&P)) has been studied for use in PP and coating material [7, 10, 11]. However, the ideal mechanical and FR properties of NR composites cannot be achieved by single-layered microencapsulation of IFR. Very few publications have been found regarding double-layered co-microencapsulation of APP and MCM-41 in NR composites. Therefore, this work aimed to establish a new method of creating an IFR system that has better mechanical and FR properties than single-layered microencapsulated IFR.

The use of intumescent additives allows the optimization of both the combustion properties and mechanical behavior of materials [6, 12]. In this paper, the double-layered co-microencapsulated APP and MCM-41 fillers (M(A&M)) with MEL-formaldehyde (MF) resin and zinc borate (ZB) (Fig. 1) was prepared by in situ polymerization. The microcapsule was then characterized by FTIR spectroscopy, laser particle size analysis, and scanning electron microscopy (SEM). The results were compared with those of APP. The use of M(A&M) as an FR in NR was evaluated by LOI and UL-94, and the mechanical properties were also studied. The thermal stability of the composite was investigated by thermogravimetry (TG) analysis [13, 14]. In addition to TG and other flame retardancy tests, detailed dynamic mechanical thermal analysis (DMTA) useful for studying the composite structure and performance was used in this study [15, 16].

Experimental

Materials

NR SMR-20 was provided by Petrochemical Co., Jilin. The commercial products APP (phase II, average degree of polymerization $n > 1000$, soluble fraction in H_2O <0.5 mass%) was supplied by Shifang Changfeng Chemical Co., Ltd., China. PER and MEL were supplied by

Sinopharm Chemical Reagent Co., Ltd. The mixture of APP, PER, and MEL was set at a mass ratio of 3:1:1, at which the FR properties were the maximum [4]. Analytical-grade zinc oxide (ZnO), stearic acid, sulfur, and other chemicals were used as received.

Spherically shaped mesoporous MCM-41 particles with uniform diameters within the range of 80–100 nm were prepared in the laboratory following a previously described method. Infrared analysis of the synthesized nanosized mesoporous MCM-41 particles has been reported in a previous work [17].

Preparation of microcapsules

Preparation of MF pre-polymer: 4.5 g of MEL, 7.0 g of 37 mass% formaldehyde solution, 0.5 g of Na_2CO_3, and 35.0 mL of deionized water were poured into a three-neck bottle and magnetically stirred. The mixed solution was heated to 80 °C and kept at that temperature for 1 h. After this step, MF pre-polymer solution was ready for microencapsulation of APP.

Preparation of microencapsulated additives: a mixture of APP and MCM-41 (40 g) with 2.0 g of 50 mass% compound dispersant solutions was first dispersed in 100 mL of ethanol and 100 mL of deionized water in a three-neck bottle and stirred for 20 min at room temperature. Then, the MF pre-polymer solution and 1.2 g of boric acid was added to the mixture, whose pH was adjusted to 5–6 with hydrochloric acid dilution. The resulting mixture was heated to 75 °C for 2 h. Then, 1 g of zinc chloride was added to the mixture and the pH was adjusted to 7–8 with 10 % NaOH solution. The mixture was kept at that temperature for 0.5 h. Then, the mixture was cooled to room temperature, filtered, washed with deionized water, and dried at 100 °C. Thus, the double-layered co-microencapsulated APP and MCM-41 fillers (M(A&M)) were finally obtained [18].

Preparation of flame-retardant NR composites

M(A&M) was mixed with other rubber compounds into NR using a laboratory two-roll mill. The components of NR compounds included PER, MEL, carbon soot, zinc oxide, stearic acid, sulfur, accelerant CZ, tetramethylthiuram disulfide, age inhibitor 4010, and electric insulating oil, which had fixed values of 13, 13, 35, 5, 4, 1.2, 0.8, 0.35, 1, 1 (phr), respectively. All NR samples were vulcanized at 145 °C in a hot press for the optimum cure time t90 determined by a GT-M2000-A rheometer (GaoTie Limited Co., Taiwan). All specimens were then cut from the vulcanized sheets and conditioned at 20 °C 24 h before testing. The formulations are provided in Table 1.

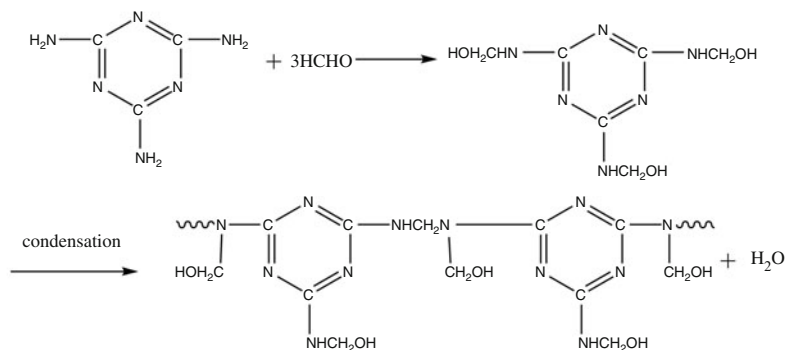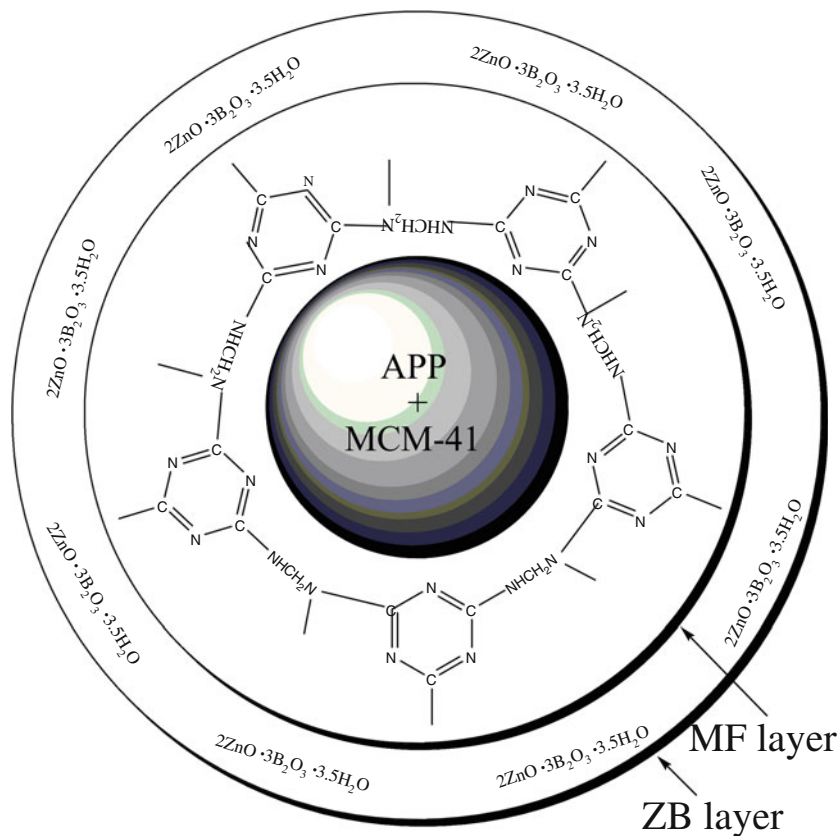**Fig. 1** Schematic and equation
of the MF layer of M(A&M)

Table 1 Formulation of flame-retardant NR composites

Sample code	NR/phr	APP/phr	MCM-41/phr	M(A&M)/phr
NR	100	–	–	–
NRAPP	100	40	–	–
NRAM 39/1	100	39	1	–
NRAM 37/3	100	37	3	–
NRAM 35/5	100	35	5	–
NRAM 30/10	100	30	10	–
NRMAPP	100	–	–	40(APP 40)
NRMAM 39/1	100	–	–	40(APP/MCM-41 39/1)
NRMAM 37/3	100	–	–	40(APP/MCM-41 37/3)
NRMAM 35/5	100	–	–	40(APP/MCM-41 35/5)
NRMAM 30/10	100	–	–	40(APP/MCM-41 30/10)

Characterization

FTIR spectroscopy

The infrared spectra of the microcapsules were obtained on a Nicolet MNGNA-IR 560 with 4 cm^{-1} resolution.

Granulometry

The mean particle size and particle size distribution of each sample were evaluated with a laser particle size analyzer (Rise-2008, Shandong, China). To prevent sample aggregation, the suspension was ultrasonically vibrated for 10 min before measurements.

SEM

The SEM images of the microcapsules and NR composites were obtained with a scanning electron microscope JEOL JSM-6360LV. The specimens were previously coated with a conductive gold layer. The samples for testing the morphology of the burnt composites were prepared using burnt samples of oxygen index. Complete burning of the samples was insured.

LOI

Limited oxygen index data were obtained at room temperature on an oxygen index instrument (JF-3) produced by Jiangning Analysis Instrument Company, China, according to ISO 4589-1984 standard. The dimensions of the specimens were $126 \times 6.5 \times 3$ mm^3.

UL-94 testing

The vertical test was carried out on a CFZ-2 type instrument (Jiangning Analysis Instrument Company, China) according to the UL-94 test standard. The specimens used had of dimensions of $126 \times 13 \times 3$ mm^3.

Tensile testing

Room-temperature tensile tests of the composites were conducted following GB/T528-1998 on an Instron 1211 testing machine at a crosshead speed of 500 mm min^{-1}.

Thermogravimetric analysis

The thermal stability of the NR composites was examined by TG using a Perkin-Elmer TGA 7 thermal analyzer at a heating rate of 10 °C min^{-1}. Nitrogen was used as a carrier gas at a constant flow rate during analysis.
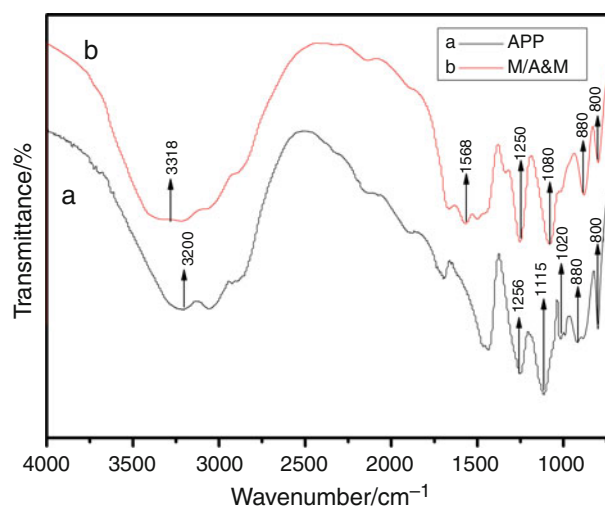
Fig. 2 FTIR spectra of APP and M(A&M)

DMTA

Dynamic mechanical properties were measured with a dynamic mechanical thermal analyzer (DMTA V, Rheometrics Science Corp.). The dynamic storage modulus was determined at a frequency of 10 Hz and a heating rate of 3 °C min^{-1} from -100 to 100 °C.

Results and discussion

Characterization of microcapsules

The FTIR spectra of APP and M(A&M) are shown in Fig. 2. The typical absorption peaks of APP were at 3200 (N–H), 1256 (P=O), 1020 (symmetric vibration of PO$_2$), 880 (P–O asymmetric stretching vibration), and 800 cm^{-1} [19]. For M(A&M), the main absorption peaks appeared at 3318, 1568, 1250, 1080, 880, and 800 cm^{-1}. The absorption at 1568 cm^{-1} was due to the ring vibration of MEL from MF resin, whereas that at the 1080 cm^{-1} band represented the asymmetric stretching vibration of Si–O–Si from MCM-41. The peak at 3318 cm^{-1} can be attributed to the O–H bond, and O–H groups can probably be attributed to the crystal water of ZB. Consequently, the spectrum of M(A&M) revealed the characteristic bands of APP/MCM-41 and the well-defined absorption peaks of MF resin and ZB.

The particle size distributions of APP and MCAPP (double-layered microencapsulated APP) are shown in Fig. 3. The mean particle size of APP increased from 14.36 to 26.54 μm after the double-layered microencapsulation of the APP with MF resin and ZB. Figure 3 clearly shows that the particle size distributions of MCAPP became more concentrated than APP without microencapsulated. The
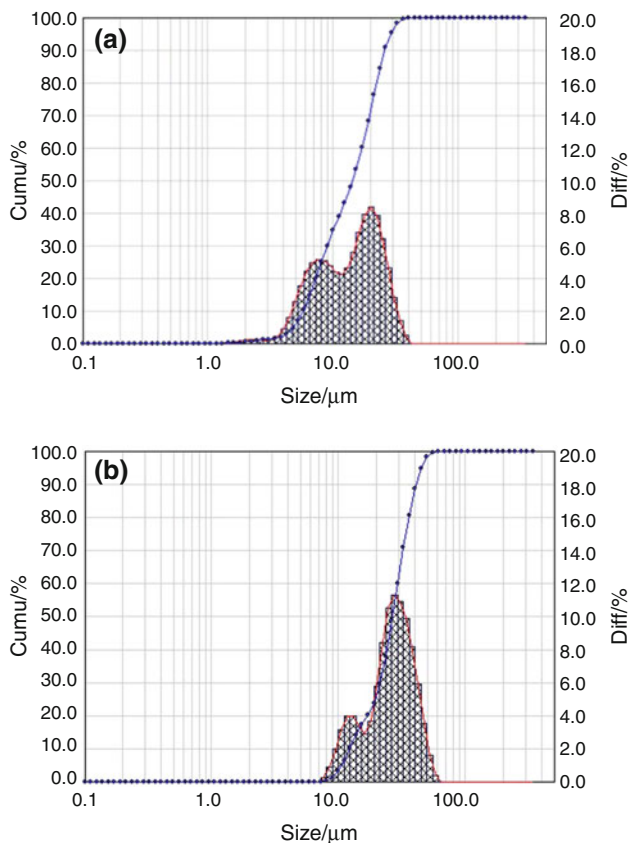
Fig. 3 Size distribution of APP (**a**) and MCAPP (**b**)

MCAPP prepared in this study had better dispersion in NR than APP when blended with NR because of the narrow particle size distribution of MCAPP. Such characteristic was expected to produce NR/MCAPP composites with better flame retardancy and mechanical properties.

The surface morphologies of the APP and MCAPP particles are shown in Fig. 4. The surface of APP particle was obviously very smooth. After double-layered microencapsulation, the morphology of the MCAPP surfaces was significantly changed and consequently showed a comparably rougher surface. This finding was probably due to the fact that the methylolation reaction in the synthesis of MF resin produced different addition products. A second step of polycondensation resulted in different degrees of polymerization of the inner layer MF resin to produce this phenomenon. Thus, double-layered microencapsulation was achieved.

Flame retardancy

Limited oxygen index and UL-94 are widely used to evaluate the flame retardancy of polymeric materials. LOI is an important parameter for testing the flammability of FR materials. LOI provides the minimum oxygen concentration by volume required to maintain the combustion of a material. The LOI and UL-94 testing results of the NR composites are presented in Table 2. The LOI of NR/M(A&M) (NRMAM) was higher than those of NR/APP/MCM-41(NRAM) composites. The NR/M(A&M) systems gave a V-1 rating when the double-layered microencapsulated ratio of APP to MCM-41 was 40:0 and 37:3. When the ratio of APP to MCM-41 was 39:1, the NR composites reached a UL-94 V-0 rating, and LOI was as high as 29.7. By contrast, the value of the NR/APP/MCM-41 system at the same additive level was only 28.4 and the UL-94 only passed the V-1 rating. Such increase may be due to the fact that when the NR composites containing M(A&M) were heated, MF resin as the inner layer of MCAPP released water vapor and NH_3 gases, which reduced the concentration of air and made the NR materials swell to form intumescent char. ZB, which is also an FR additive that can serve as a Lewis acid, acted in synergy with IFR additives as the outer layer of M(A&M) and catalyzed the esterification reaction of IFR to form a stronger intumescent char.

The findings revealed that regardless of the occurrence of APP and MCM-41 double-layered microencapsulation, LOI and UL-94 reached the maximum values when the ratio of APP to MCM-41 was 39:1. A suitable APP/MCM-41 ratio in the system was very important for the enhancement of FR properties in NR composites. This phenomenon was probably due to the synergistic effect between IFR and MCM-41. Moreover, MCM-41 can

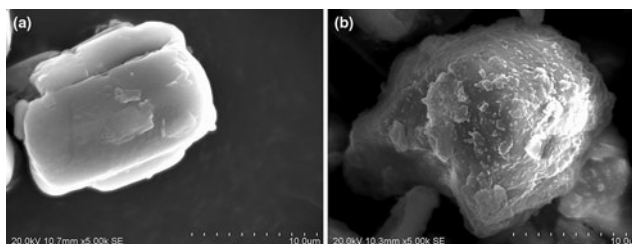**Fig. 4** SEM images of APP (**a**) and MCAPP (**b**) particles

Table 2 Flame retardancy and mechanical property of flame-retardant NR composites

Flame-retardant composite	Flame retardancy		Mechanical property	
	LOI/%	UL-94	Tensile strength/MPa	Elongation at break/%
NR	16	No rating	21.9	413.5
NRAPP	25.8	No rating	5.9	268.4
NRAM 39/1	28.4	V-1	7.4	295.1
NRAM 37/3	27.6	No rating	7.4	301.1
NRAM 35/5	27.7	No rating	6.4	301.8
NRAM 30/10	26.1	No rating	8.0	240.0
NRMAPP	28.2	V-1	7.2	298.2
NRMAM 39/1	29.7	V-0	8.1	313.1
NRMAM 37/3	29.0	V-1	8.0	302.8
NRMAM 35/5	28.4	No rating	7.8	304.7
NRMAM 30/10	26.5	No rating	9.0	298.4

reduce the amount of amorphous char protecting and strengthening the intumescent char. The above results showed that the presence of MF resin and ZB outside APP and MCM-41 enabled M(A&M) to be an effective flame-retardant in NR compared with APP/MCM-41. Double-layered microencapsulation and the synergist MCM-41 can remarkably enhance the FR properties of NR composites.

Mechanical properties

The mechanical properties of NR and FR NR composites are shown in Table 2. The tensile strength value and elongation at break were 5.9 MPa and 268.4 % for the NR/APP system, as well as 21.9 MPa and 413.5 % for NR, respectively. The addition of IFR filler markedly decreased the mechanical properties of the NR composites. After microencapsulation, the tensile strength and elongation at break evidently increased compared with un-microencapsulated samples. This finding was due to the fact that ZB as the outer layer of double-layered microencapsulation is inorganic and can reinforce the strength of microencapsulation. The maximum tensile strength value of M(A&M) (NRMAM 30/10) and the maximum elongation at break of NR/M(A&M) (NRMAM 39/1) reached the maximum at 9.0 MPa and 313.1 %, respectively. These obvious improvements in tensile strength and elongation at break were probably due to the stiffness of MCM-41, which resulted in the reinforcement of NR composites. MCM-41 can also adsorb H_2S that was emitted during vulcanization, and can thus decrease the quantity of heat that may improve the average vulcanization temperature. This phenomenon can prevent the untime sulfation and decrease in the cross-linking degree of the NR composites [20].

Morphology of burnt composites

The SEM image of burnt NR/APP (NRAPP), NR/MCAPP (NRMAPP), NR/M(A&M) (NRMAM 39/1), and NR/APP/MCM-41(NRAM 39/1) composites are shown in Fig. 5. Without double-layered microencapsulation, a relative loose structure, cracks, cavities, and some incomplete hollow fractured bubbles can be observed on the surface of the char residue in NR/APP. Consequently, heat and flammable volatiles can easily penetrate through the char layer into the interior of the composites during combustion. After being double-layered microencapsulated with MF resin and ZB, NR/MCAPP formed a relatively complete char layer that had fewer, smaller cracks and cavities than NR/APP. This finding indicated that double-layered microencapsulation was effective in forming a stronger char layer. Regarding the NR/M(A&M) composite, the microstructure of the char residue displayed a more compact structure and almost no cavities compared with the samples without MCM-41 (Fig. 5b). This result was due to the ability of MCM-41 to effectively slow down the degradation of underlying materials and stop the transfer of heat and flammable volatiles. For NR/APP/MCM-41, the char layer non-uniformly inflated but a compact structure was formed. The bigger inflated bubble can easily fracture. Analysis of these images suggested that double-layered microencapsulation and the addition of MCM-41 positively affected the FR properties of NR composites.

Thermal stability

The TG curves of NR and FR NR composites are shown in Fig. 6. The related TG data are presented in Table 3.

Fig. 5 SEM images of flame-retardant composites (×500): **a** NRAPP, **b** NRMAPP, **c** NRMAM 39/1, and **d** NRAM 39/1
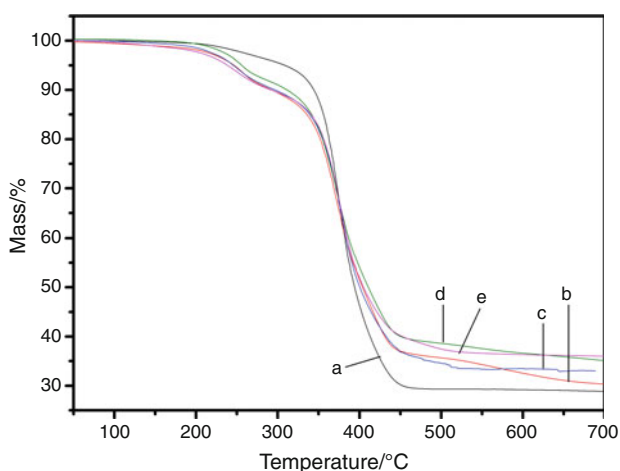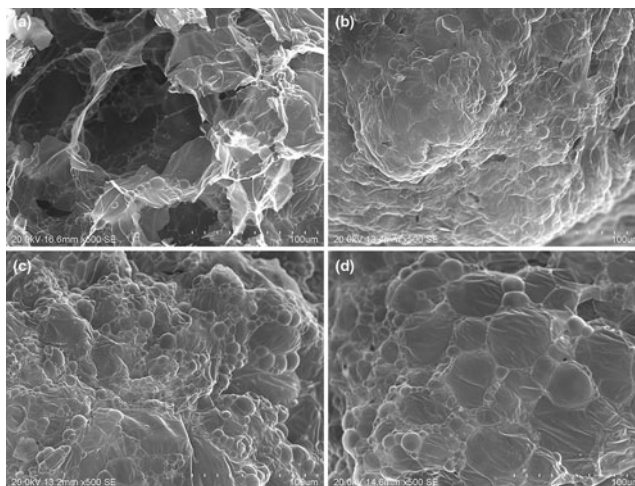

Fig. 6 TG curves of **a** NR, **b** NRAPP, **c** NRMAPP, **d** NRMAM 39/1, and **e** NRAM 39/1

Thermal degradation of pure NR under N_2 atmosphere involved two steps. The decomposition of NR began at about 220 °C and steadily decomposed at 470 °C.

The addition of fillers to NR significantly decreased T10 % compared with pure NR because of the thermal degradation of IFR. The decomposition processes of NR/MCAPP were similar to those of NR/APP, but NR/MCAPP was more stable when the temperature exceeded 520 °C. This phenomenon may be due to the fact that the MF shell materials serving as char source and gas source, as well as ZB that served as the Lewis acid, produced a synergism with the FR additives and catalyzed the esterification reaction of IFR, thereby forming a stronger intumescent char.

The NR/M(A&M) composite showed T50 % of 411 °C, which was 17 and 12 °C higher than NR and NR/MCAPP, respectively. The degradation of NR/M(A&M) ended with a mass loss of 36.61 % higher than the other samples. The samples with MCM-41 additive had higher T50 % and residues than the samples without MCM-41. Hence, MCM-41 dispersed in the composites possessed high thermal stability and good barrier properties, which may slow down heat transmission to the polymer, consequently delaying the decomposition of the composites [21]. Therefore, the thermal stability of the NR/M(A&M) composite was remarkably better than those of the other samples.

DMTA

The storage modulus and tan δ of NR and FR NR composites are shown in Figs. 7, 8, respectively. NR/M(A&M) had the highest storage modulus among all samples in all temperature regions probably because the inorganic ZB outer shell of the double-layered microencapsulated APP and rigid MCM-41 in the microencapsulation imparted certain stiffness behaviors to the NR composites. The storage modulus measured the recoverable strain energy in deformed specimens, so it reflected the elastic modulus of materials. The glass transition temperature (T_g) of the samples determined from the temperature at the maximum tan δ were as follows: NR/APP (−54.29 °C), NR/MCAPP (−52.42 °C), NR/M(A&M) (−51.38 °C), and NR/APP/MCM-41 (−51.16 °C). T_g of NR/MCAPP and NR/M(A&M) can be observed to shift toward high temperature because the comparably rougher surface of the microencapsulated APP and its rigid shell limited the mobility of

Table 3 TG data of flame-retardant NR composites

Sample	$T_{10\%}/°C$[a]	$T_{20\%}/°C$[b]	$T_{50\%}/°C$[c]	Mass/ % at 600 °C
NR	308.43	362.61	394.06	29.18
NRAPP	246.42	352.07	403.77	32.54
NRMAPP	245.57	354.89	400.56	33.50
NRMAM 39/1	255.71	355.35	411.00	36.61
NRAM 39/1	238.38	356.22	405.07	36.31

[a] Temperature at 10 % mass loss

[b] temperature at 20 % mass loss
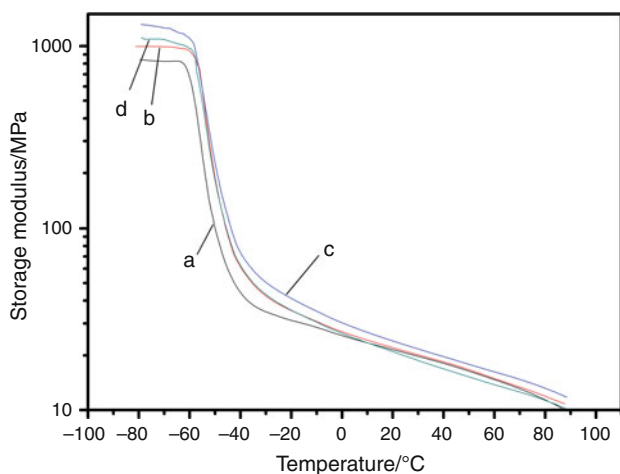
[c] temperature at 50 % mass loss

Fig. 7 Temperature dependence of tan δ of NR and FR NR composites: **a** NRAPP, **b** NRMAPP, **c** NRMAM 39/1, and **d** NRAM 39/1
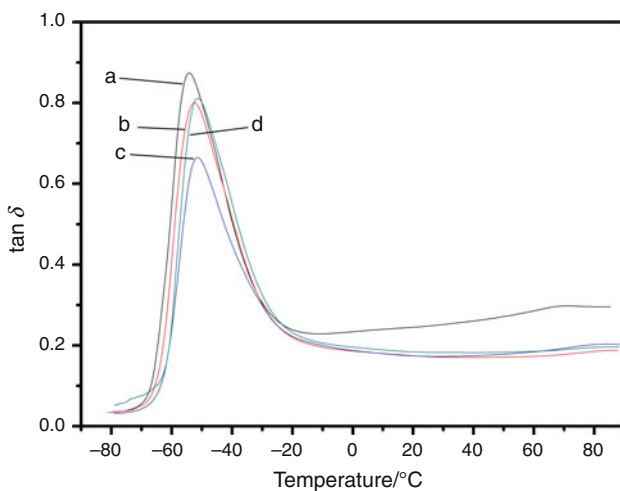

Fig. 8 Temperature dependence of storage modulus of NR and FR NR composites: **a** NRAPP, **b** NRMAPP, **c** NRMAM 39/1, and **d** NRAM 39/1

the polymer chains. T_g of NR/APP/MCM-41 increased to the maximum unlike NR/MCAPP and NR/M(A&M), which was probably due to the strong interaction formed by

rigid MCM-41 with the NR matrix such as physical and chemical adsorption to reduce chain mobility. A similar result has been reported by Ľalíková et al. [22].

Conclusions

Double-layered co-microencapsulated APP and mesoporous MCM-41 with MF resins and ZB were successfully prepared by in situ polymerization. The microcapsules demonstrated excellent particle size distribution and morphology. The result showed that NR M(A&M) (NRMAM 39/1) had a remarkable improvement in both flame retardancy and mechanical properties. An increased T_g, a lowered tan δ peak value, and the highest storage modulus were obtained in (NRMAM 39/1) compared with the other samples because both MF resin and ZB as the double shell of the microcapsules produced a synergism with IFR to form a stronger intumescent char. When MCM-41 was added to the microcapsules, it effectively enhanced the flame retardancy, mechanical, and thermal properties of NR composites by acting as a synergistic agent compared with the NR/MCAPP system. In summary, the NR/M(A&M) (NRMAM 39/1) can be a promising formulation for flame-retardant NR composites.

References

1. Huang GB, Li YJ, Han L, Gao JR, Wang X. A novel intumescent flame retardant-functionalized montmorillonite: preparation, characterization, and flammability properties. Appl Clay Sci. 2011;51:360–5.
2. Wang DL, Liu Y, Wang DY, Zhao CX, Mou YR, Wang YZ. A novel intumescent flame-retardant system containing metal chelates for polyvinyl alcohol. Polym Degrad Stab. 2007;92: 1555–64.

3. Carli LN, Roncato CR, Zanchet A, Mauler RS, Giovanela M, Brandalise RN, Crespo JS. Characterization of natural rubber nanocomposites filled with organoclay as a substitute for silica obtained by the conventional two-roll mill method. Appl Clay Sci. 2011;52:56–61.

4. Wang JC, Yang K, Zheng XY. Studies on the effect of 4A zeolite on the properties of intumescent flame-retardant agent filled natural rubber composites. J Polym Res. 2009;16:427–36.

5. Wang BB, Wang XF, Tang G, Shi YQ, Hu WZ, Lu HD, Song L, Hu Y. Preparation of silane precursor microencapsulated intumescent flame retardant and its enhancement on the properties of ethylene–vinyl acetate copolymer cable. Compos Sci Technol. 2012;72:1042–8.

6. Wang N, Gao N, Jiang S, Fang QH, Chen EF. Effect of different structure MCM-41 fillers with PP-g-MA on mechanical and crystallization performances of polypropylene. Compos B. 2011;42:1571–7.

7. Sun LS, Qu YT, Li SX. Co-microencapsulate of ammonium polyphosphate and pentaerythritol in intumescent flame-retardant coatings. J Therm Anal Calorim. 2013;111:1099–106.

8. Saihi D, Vroman I, Giraud S, Bourbigot S. Microencapsulation of ammonium phosphate with a polyurethane shell. Part II. Interfacial polymerization technique. React Funct Polym. 2006;66:1118–25.

9. Wu K, Wang ZZ, Hu Y. Microencapsulated ammonium polyphosphate with urea–melamine–formaldehyde shell: preparation, characterization, and its flame retardance in polypropylene. Polym Adv Technol. 2008;19:1118–25.

10. Wang ZZ, Wu K, Hu Y. Study on flame retardance of co-microencapsulated ammonium polyphosphate and dipentaerythritol in polypropylene. Polym Eng Sci. 2008;48:2426–31.

11. Chen XL, Jiao CM. Study on flame retardance of co-microencapsulated ammonium polyphosphate and pentaerythritol in polypropylene. J Fire Sci. 2010;28:509–21.

12. Wang N, Zhang J, Fang QH, Hui D. Influence of mesoporous fillers with PP-g-MA on flammability and tensile behaviour of polypropylene composites. Compos B. 2012;44:467–71.

13. Supriya N, Catherine KB, Rajeev R. DSC-TG studies on kinetics of curing and thermal decomposition of epoxy–ether amine systems. J Therm Anal Calorim. 2013;112:201–8.

14. Sharma R, Sharma N. A thermal behaviour and structural study of bis(hydroxamato)oxovanadium(IV) complexes. J Therm Anal Calorim. 2013;112:25–30.

15. Nigam V, Setua DK, Mathur GN. Characterization of rubber epoxy blends by thermal analysis. J Therm Anal Calorim. 2001;64:521–7.

16. Ochigbo SS, Luyt AS, Focke WW. Latex derived blends of poly (vinyl acetate) and natural rubber: thermal and mechanical properties. J Mater Sci. 2009;44:3248–54.

17. Wang N, Shao YW, Shi ZX, Zhang J, Li HW. Preparation and characterization of epoxy composites filled with functionalized nano-sized MCM-41 particles. J Mater Sci. 2008;43:3683–8.

18. Lu JP, Wu Q, Qu BJ. Preparation of microcapsulated red phosphorus coated with melamine-formaldehyde resin/zinc borate and its applications in flame retardant polyolefins. J Funct Polym. 2003;16:507–12.

19. Bugajny M, Bourbigot S, Le Bras M. The origin and nature of flame retardance in ethylene-vinyl acetate copolymers containing hostaflam AP 750. Polym Int. 1999;48:264–70.

20. Wang JC, Chen YH. Effect of microencapsulation and 4A zeolite on the properties of intumescent flame-retardant natural rubber composites. J Fire Sci. 2008;25:153–71.

21. Wang N, Yu S, Zhang J, Fang QH, Chen EF. Effect of nanosized mesoporous MCM-41 (with template) material on properties of natural rubber nanocomposites. Plast Rubber Compos. 2011;40:402–6.

22. Ľalíková S, Pajtášová M, Chromčíková M, Liška M, Šutinská V, Olšovský M, Ondrušová D, Mojumdar SC. Investigation of natural rubber composites with addition of montmorillonite fillers using thermal analysis. J Therm Anal Calorim. 2011;104:969–73.